Doctoral Dissertation (Censored)
博士論文（要約）

Climatology and interannual variability of stratospheric planetary waves in the Southern Hemisphere and their connection to the troposphere

（南半球成層圏におけるプラネタリー波のクライマトロジー及び年々変動とその対流圏との関係）

A Dissertation Submitted for the Degree of Doctor of Philosophy
July 2019
令和元年 **7** 月博士（理学）申請

Department of Earth and Planetary Science,
Graduate school of Science, The University of Tokyo
東京大学　大学院理学系研究科　地球惑星科学専攻

Soichiro Hirano
平野 創一朗

Abstract

Planetary-scale Rossby waves in the wintertime polar stratosphere and associated dynamical phenomena are introduced in chapter 1. The wintertime polar stratosphere is dominated by planetary waves propagating from the troposphere. Amplitudes of stratospheric planetary waves in winter are generally smaller in the Southern Hemisphere (SH) than in the Northern Hemisphere (NH) due to differences in amplitudes of the geographical asymmetries. As a result, significant interhemispheric differences in dynamical phenomena associated with planetary waves are observed in the wintertime polar stratosphere. For example, the stratospheric final warming (SFW), which is the breakdown of the polar vortex, occurs approximately one month later in the SH than in the NH.

Planetary waves with large amplitudes in the SH polar stratosphere are quasi-stationary waves with zonal wavenumber 1 ($s = 1$ QSWs; s is zonal wavenumber) and transient waves with zonal wavenumber 2 ($s = 2$ TWs). Climatological seasonal evolution of the planetary-wave amplitudes in the SH stratosphere is already shown by previous studies using data for a limited time period. However, cause of the seasonal variation of stratospheric planetary-wave amplitudes is still not clear. Moreover, although it has already been confirmed by previous studies that SFWs occur earlier when stratospheric wave activity is larger, detailed tropospheric conditions leading to earlier SFWs are still not elucidated well. The present study investigates climatology and interannual variability of planetary waves in the SH stratosphere and their connection to the troposphere. The analysis is focused on planetary waves in the troposphere and wave transmission properties of the mean flow through which planetary waves propagate. Refractive index (n) squared is used to

diagnose the wave transmission properties of the mean flow. Reanalysis dataset (MERRA-2) for 38 years from 1980 to 2017 is mainly used.

In chapter 2, climatological seasonal evolution of planetary-wave amplitudes in the SH stratosphere is shown. The climatology for 38 years obtained in this study is compared to that shown by the previous studies. This is because the time period of data used for climatology by previous studies is relatively short, which may lead to spurious climatology affected by a certain phase of the interannual variability. Cause of the climatological seasonal variation of planetary-wave amplitudes in the stratosphere is examined in terms of the climatological seasonal variation of planetary-wave amplitudes in the troposphere and distribution of n^2 in the stratosphere. In addition, the relation of the distribution of n^2 with the structure of the polar night jet is investigated. Results of the analysis for $s = 1$ QSWs and $s = 2$ TWs are shown.

For $s = 1$ QSWs, seasonal evolution of the stratospheric wave amplitudes is different between above and below 3 hPa. The wave amplitudes above 3 hPa attain a local maximum in autumn, a local minimum in midwinter, and a maximum in spring. On the other hand, the wave amplitudes below 3 hPa gradually increase from early winter and are maximized in spring. A local maximum in the middle stratosphere in early winter observed in climatology shown by previous studies is not seen. The midwinter maximum in the middle stratosphere shown by the previous studies reflects significantly large amplitudes of $s = 1$ QSWs in a year during time period analyzed by previous studies.

Possible cause of the climatological seasonal evolution of $s = 1$ QSW amplitudes in the stratosphere is examined. A region which is largely occupied by negative n^2 is observed in midwinter. This is consistent with the local minimum of the wave amplitudes in midwinter. On the other hand, in the lower stratosphere, n^2 is largely positive from early winter to spring. The wave amplitudes in the troposphere gradually increase from early winter and are maximized in spring. Thus, it is suggested that the gradual increase of the stratospheric wave amplitudes below 3 hPa is due to that of tropospheric wave amplitudes. The maximum of the wave amplitudes in spring in the whole stratosphere is likely caused by the maximum in tropospheric wave activity.

For $s = 2$ TWs, stratospheric wave amplitudes gradually increase from early winter and attain a maximum in late winter. This is almost the same as climatology shown by a previous study. It is suggested that the gradual increase in stratospheric wave amplitudes from early to mid-winter is caused by both gradual increase in tropospheric wave activity and latitudinal widening of lower stratospheric positive n^2. The maximum of stratospheric wave amplitudes in late winter is likely associated with tropospheric wave activity which attains the maxima twice in mid- and late winter, and larger areas of positive n^2 in the middle and upper stratosphere in late winter than in midwinter.

In chapter 3, interannual variability of SFW date in the SH is investigated in terms of difference in stratospheric wave activity between early and late SFW years. The analysis is focused on $s = 1$ QSWs because their amplitudes are the largest among extratropical planetary waves in the SH stratosphere, and attain a maximum during the austral spring. Stratospheric $s = 1$ QSW activity is larger in early-SFW years than in late-SFW years in late winter and spring before SFW. Larger wave forcing due to $s = 1$ QSWs is observed in early-SFW years in the stratosphere. This likely leads to advanced seasonal evolution of the polar night jet, and hence early SFWs. The larger $s = 1$ QSW activity in early-SFW years is also observed in the troposphere. From the troposphere to the stratosphere, larger upward Eliassen-Palm flux is observed in early-SFW years. These results indicate that the larger stratospheric $s = 1$ QSW activity originates in the troposphere. It is shown by examining the distribution of n^2 that more favorable conditions for $s = 1$ stationary waves to propagate from the

troposphere into the stratosphere in early-SFW years than in late-SFW years are found at high latitudes. This indicates contribution of the difference in wave transmission properties of the mean flow to the larger stratospheric $s = 1$ QSW activity. In addition, it is suggested that the difference in wave transmission properties of the mean flow between early- and late-SFW years comes from advanced seasonal evolution of the polar night jet in early-SFW years.

Next, cause of the larger amplitudes of tropospheric $s = 1$ QSWs in early-SFW years is explored. The analysis is focused on Rossby wave source (RWS) at low latitudes and the background flow in the troposphere because they may mainly affect the amplitudes of tropospheric $s = 1$ QSWs. Significant differences in the RWS at low latitudes and the background flow between early- and late-SFW years are observed. Difference in $s = 1$ steady response to the RWS at low latitudes and the background streamfunction is calculated using a linear barotropic model. The difference in $s = 1$ response is compared to difference in $s = 1$ stationary waves in MERRA-2 at high latitudes. Their longitudinal phase structures are similar. It is indicated that the cause of the larger amplitudes of $s = 1$ response in early-SFW years is different between late winter and spring seasons. Difference in RWS at low latitudes matters in late winter, while difference in background wind with zonally asymmetric structure is important in spring.

The above results indicate that the larger amplitudes of $s = 1$ QSWs in early-SFW years are caused by stationary Rossby waves which originate in low latitudes. It is shown that synoptic-scale waves may also contribute to the larger amplitudes of $s = 1$ QSWs in early-SFW years.

In chapter 4, summary and concluding remarks are given.

要旨

第 1 章では、冬季極域成層圏におけるプラネタリー波及びそれに関連する力学現象に関する導入を行った。冬季極域成層圏では、対流圏から伝播する惑星規模のロスビー波が卓越する。プラネタリー波の振幅は北半球に比べ南半球の方が小さく、これは地形や非断熱加熱の東西非一様性の大きさの違いによると考えられている。この結果、プラネタリー波に関連した力学現象に南北半球間で違いが見られる。例えば、冬季極渦の消滅に対応する最終昇温のタイミングは、北半球に比べて南半球の方が 1 か月程度遅い。

南半球で卓越するプラネタリー波は、東西波数 1 の準停滞波（quasi-stationary waves with zonal wavenumber 1; 以下、$s = 1$ QSWs）と東西波数 2 の移動性の波（transient waves with zonal wavenumber 2; 以下、$s = 2$ TWs）である。南半球成層圏におけるプラネタリー波の振幅のクライマトロジカルな季節進行は限られた期間に対し既に示されているが、その原因は必ずしも明らかでない。また、最終昇温のタイミングの年々変動と成層圏における波活動との関係は既に示されているが、成層圏での波活動を決める対流圏の具体的な条件は示されていない。そこで、本研究では、南半球成層圏におけるプラネタリー波のクライマトロジー及び年々変動とその対流圏との関係を調べる。そのために、対流圏のプラネタリー波の振幅と平均流に関連したプラネタリー波の伝播特性に着目する。伝播特性を診断するために、refractive index (n) の 2 乗を用いる。解析には、1980 年から 2017 年までの 38 年分の再解析データ (MERRA-2) を主に用いる。

第 2 章では、南半球成層圏におけるプラネタリー波のクライマトロジーを示す。これを先行研究で示されたものと比較する。先行研究で使用されたデータの期間が短く、年々変動を十分除いた気候値になっていない可能性があるからである。成層圏におけるプラネタリー波の振幅の季節進行の要因を、対流圏のプラネタリー波の振幅と成層圏におけるn^2の分布の観点から調べた。さらに、n^2の分布を極夜ジェットの構造と関係づけた。ここでは、$s = 1$ QSW と$s = 2$

TW の結果を示す。

成層圏における$s=1$ QSW の振幅の季節進行は、3 hPa より上層と下層では異なる。3 hPa より上層においては、秋に極大、真冬に極小、春に最大となる。一方、3 hPa より下層の振幅は、冬の初めから徐々に増え、春で最大となる。先行研究で指摘された初冬の極大は見られなかった。これは、真冬に年々変動が大きく、先行研究の解析期間に振幅の大きい年が偏って含まれているためである。

成層圏における$s=1$ QSW の振幅の季節進行の要因を調べた。成層圏界面付近では、n^2が負となる領域が真冬に見られた。これは、3 hPa より上層における真冬の振幅の極小と定性的に整合している。一方、下部成層圏では、n^2が冬の初めから春にかけて正であった。また、対流圏の振幅は冬の初めから徐々に増え、春に最大となっていた。したがって、3 hPa より下層における振幅の増大は、主に対流圏における振幅の増大によると考えられる。また、成層圏全体における春の振幅の最大は、対流圏の振幅の最大と対応している。

次に、$s=2$ TW の結果を述べる。成層圏の振幅は冬の初めから徐々に増え、冬の終わりに最大となる。これは、先行研究で示されたクライマトロジーの特徴もほぼ同じであった。冬の初めから真冬にかけての振幅の増大は、対流圏の振幅の増大及びn^2が正の領域の緯度方向の幅が増えることで説明できる。一方、冬の終わりの振幅の最大は、対流圏の振幅が真冬と冬の終わりに最大となること、及び中上部成層圏でn^2が正となる領域が真冬に比べて冬の終わりの方が大きいことと対応している。

第 3 章では、南半球の最終昇温日の年々変動を成層圏における波活動の観点から、最終昇温日が早い年と遅い年の差を計算することにより調べる。特に、振幅が南半球成層圏で最も大きく、冬の終わりから春にかけて最大となる$s=1$ QSW に着目する。まず、$s=1$ QSW の振幅の差を調べたところ、最終昇温が起こる前の冬の終わりと春季には、最終昇温が遅い年に比べて早い年の方が、成層圏における$s=1$ QSW の振幅が大きいことがわかった。成層圏では$s=1$ QSW による波強制が早い年の方が大きかった。これにより、極夜ジェットの季

節進行が早められ、最終昇温が早く起こると考えられる。一方、$s = 1$ QSW の振幅は対流圏でも早い年の方が大きいことがわかった。Eliassen-Palm flux (以下、E-P flux) の差を調べたところ、対流圏から成層圏にかけて上向き E-P flux が早い年の方が大きかった。これらの事実は、成層圏における$s = 1$ QSW の振幅の差の起源が対流圏にあることを示唆する。次に、n^2の分布を調べたところ、早い年の方が$s = 1$の定在波が対流圏から成層圏に伝播しやすいことがわかった。この伝播特性の差も、成層圏で$s = 1$ QSW の振幅が早い年の方が大きいことに寄与すると考えられる。また、この伝播特性の差は、極夜ジェットの季節進行の差によることも確認した。

次に、早い年の方が対流圏における$s = 1$ QSW の振幅が大きい要因を調べる。まず、$s = 1$ QSW の振幅を決めると思われる、対流圏低緯度の Rossby wave source (以下、RWS) と背景風を解析したところ、早い年と遅い年で顕著な違いが見られた。そこで、線形順圧モデルを用いて、低緯度の RWS 及び背景風に対する$s = 1$の応答の差を計算した。高緯度における$s = 1$の応答の差と MERRA-2 における$s = 1$の定在波の差を比べたところ、経度構造が類似していた。さらに、早い年に$s = 1$の応答の振幅が大きい要因が冬の終わりと春では異なることを示唆する結果を得た。冬の終わりには低緯度の RWS の差が、春には背景風の差が、早い年における$s = 1$ QSW の振幅の増大に主に寄与することがわかった。

以上の結果は、早い年の方が$s = 1$ QSW の振幅が大きいことが、低緯度から高緯度へ伝播する停滞性のロスビー波によることを示唆する。また、総観規模波が、早い年に$s = 1$ QSW の振幅が大きいことに対して寄与する可能性も示された。

第 4 章では、全体をまとめ、今後の展望を述べた。

Contents

Chapter 1
General introduction

1.1 Planetary waves in the wintertime polar stratosphere

The wintertime polar stratosphere is dominated by planetary-scale Rossby waves propagating from the troposphere (Fig. 1.1; Plumb 2002). This is because small-scale Rossby waves cannot propagate upward into the stratosphere due to filtering by background wind (Charney and Drazin 1961). The tropospheric sources of stratospheric planetary waves are associated with geographical asymmetries such as topography and spatially inhomogeneous heating which mainly comes from land-sea contrasts (Scinocca and Haynes 1998). Amplitudes of stratospheric planetary waves in winter are generally larger in the Northern Hemisphere (NH) than in the Southern Hemisphere (SH) due to interhemispheric difference in amplitudes of the geographical asymmetries (Leovy and Webster 1976). As a result, significant interhemispheric differences in dynamical phenomena associated with planetary waves are observed in the wintertime polar stratosphere. The first example is extent of ozone loss. The polar temperature is lower in the SH because heat transport by planetary wave forcing (Fig. 1.1) is weaker. The lower temperature leads to more frequent emergence of polar stratospheric clouds (PSCs). Ozone is destroyed primarily by chlorine radicals converted from the stable chlorine reservoirs HCl and $ClONO_2$ through heterogeneous reactions on PSC particles (Solomon 1999; Pitts et al. 2018). Thus, more intense ozone loss, which often leads to formation of the ozone hole, is observed in the SH.

The second example is frequency of stratospheric sudden warming (SSW). During SSW events, the polar vortex displaces or splits into two, and then completely breaks

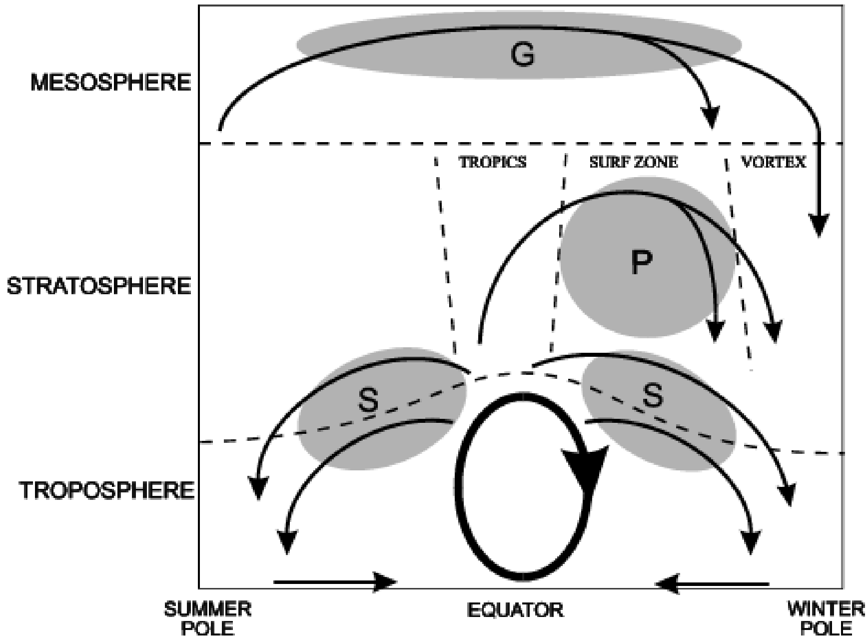

Fig. 1.1 Schematic of the residual mean flow in the atmosphere. The heavy ellipse denotes the thermally-driven Hadley circulation in the troposphere. The shaded regions (labelled “S”, “P”, and “G”) denote where breaking of waves (synoptic- and planetary-scale waves, and gravity waves, respectively) occurs, which is responsible for driving respective branches of the stratospheric and mesospheric circulation. Adopted from Plumb (2002).

down in midwinter. Subsequently, the polar vortex gradually recovers (Charlton and Polvani 2007; Matthewman et al. 2009; Mitchell et al. 2013). Due to the interhemispheric difference in stratospheric planetary-wave activity, the frequency of SSW in the NH is approximately six events per decade (Palmeiro et al. 2015; Butler et al. 2017) while SSW in the SH is observed only once in 2002 since the beginning of Antarctic record in the late 1950s (Charlton et al. 2005; Kruger et al. 2005; Newman and Nash 2005; Roscoe et al. 2005). Time series of climatological zonal-mean zonal wind at 10 hPa in the SH and NH is shown in Fig. 1.2. In midwinter, stratospheric zonal wind is much stronger in the SH. The interhemispheric difference in the stratospheric zonal wind reflects those in the frequency of SSWs. The last example is timing of stratospheric final warming (SFW) in spring. During SFWs, seasonal transition from strong circumpolar westerlies characterized by the polar vortex during winter to weak

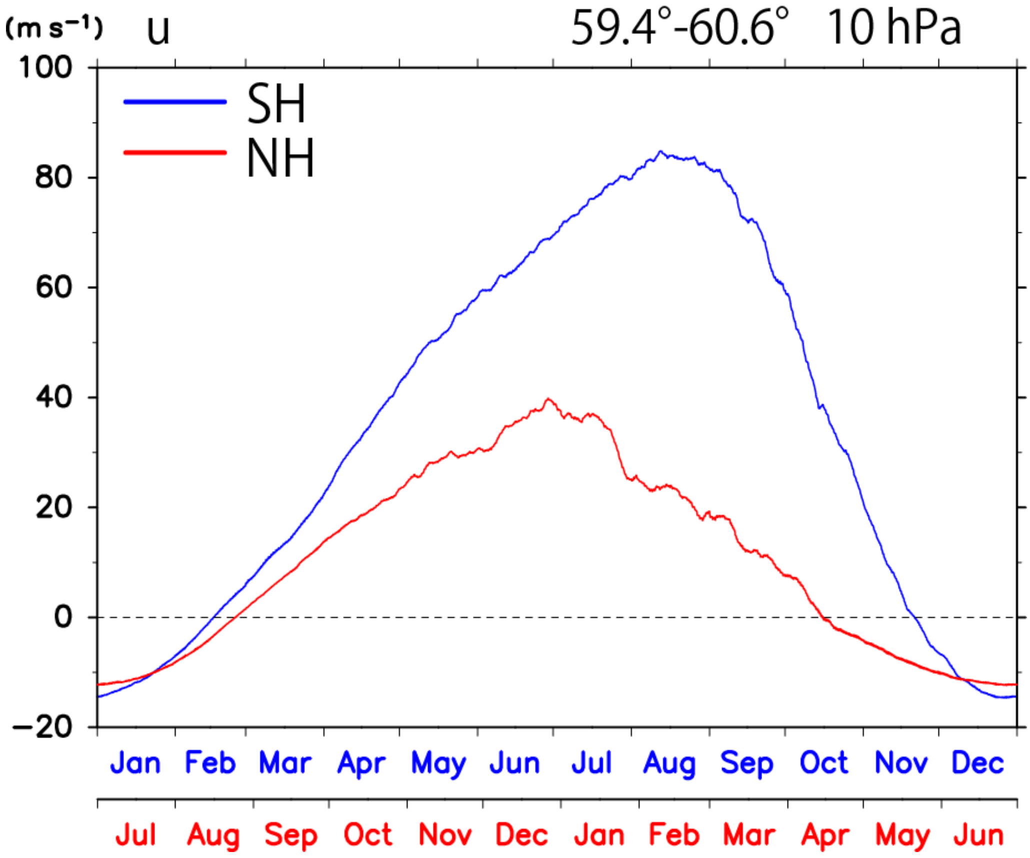

Fig. 1.2 Time series of climatological zonal-mean zonal wind ($\bar{u}$) at 10 hPa averaged over a latitudinal range of 59.375°–60.625°. Blue and red curves denote $\bar{u}$ in the SH and NH, respectively. Note that calendar months in the time axis for the NH is lagged by 6 months relative to that for the SH. The figure is made using MERRA-2 from 1980 to 2017.

circumpolar easterlies characterized by an anticyclone during summer occurs (Andrews et al. 1987). SFWs should be distinguished from SSWs because westerlies recover after the weakening and/or collapse of the polar vortex during SSWs (Hu et al. 2014). SFWs occur later in the SH than in the NH mainly due to the interhemispheric difference in stratospheric planetary-wave activity (Fig. 1.2; Black et al 2006; Black and McDaniel 2007a; 2007b).

In the SH, quasi-stationary waves with zonal wavenumber 1 ($s = 1$ QSWs; s is zonal wavenumber) have the largest amplitude among stratospheric planetary waves (Randel 1988; Quintanar and Mechoso 1995a). The amplitude of $s = 1$ QSWs attains its maximum in the austral spring along with a secondary smaller maximum in midwinter. A local minimum is sandwiched by the two maxima (Labitzke 1980; Hirota et al. 1983). The seasonal evolution of amplitudes of stratospheric $s = 1$ QSW in the SH has been examined from the different viewpoints (Scott and Haynes 2002). Randel (1988) showed seasonal evolution of refractive index squared (n^2) to diagnose the influence of zonal-mean zonal wind on the propagation of $s = 1$ stationary waves in the meridional cross section. Refractive index squared for waves with phase speed c_p and zonal wavenumber s is expressed as

$$n^2 = \frac{\bar{q}_\phi}{a\left(\bar{u} - c_\mathrm{p}\right)} - \frac{s^2}{a^2 \cos^2 \phi} - \frac{f^2}{4N^2H^2}, \tag{1.1}$$

where

$$\frac{\bar{q}_\phi}{a} = \frac{2\Omega \cos \phi}{a} - \left(\frac{(\bar{u} \cos \phi)_\phi}{a^2 \cos \phi}\right)_\phi - \frac{1}{\rho_0}\left(\frac{\rho_0 f^2}{N^2}\bar{u}_z\right)_z \tag{1.2}$$

is gradient of zonal-mean quasi-geostrophic (QG) potential vorticity (PV); $\bar{u}$ is zonal-mean zonal wind; ϕ is latitude; z is height; ρ_0 is the basic density; f is the Coriolis parameter; N is the buoyancy frequency; a is the Earth's radius; H is the scale height; and subscripts refer to derivatives with respect to the given variable. An equation obtained by substituting a wave form solution into a linearized QGPV equation is similar to the equation for two-dimensional sound or light waves in a medium of varying refractive index n. By insights from the theory of acoustics or optics, waves are expected to propagate in regions with positive n^2 and avoid regions with negative n^2, so that they tend to propagate towards regions with large positive n^2 (Matsuno 1970; Andrews et al. 1987).

Randel (1988) found that the largest value of n^2 is observed in the lower stratosphere when amplitudes of $s = 1$ QSWs attain a local minimum. The two maxima of amplitudes of $s = 1$ QSWs are not in agreement with seasonal changes in

n^2. Wirth (1991) solved the linear steady-state QG equation with a prescribed zonally symmetric basic state and a stationary $s = 1$ forcing at the lower boundary based on climatological monthly mean zonal winds and geopotential amplitudes. It was shown that the seasonal evolution of $s = 1$ QSW amplitudes is roughly consistent with that of n^2, although the secondary maximum in midwinter is not reproduced in their model.

Other mechanisms for the twin maxima observed in the amplitudes of $s = 1$ QSWs have been proposed in the literature. Wakata and Uryu (1987) and Yoden (1990) interpreted the twin maxima of $s = 1$ QSW amplitudes as transitions between separate stable solution branches of a steady system, in which the strength of radiative basic-state wind is an external bifurcation parameter. Scott and Haynes (2002) suggested that resonance with the lower boundary forcing in midwinter and spring leads to the twin maxima.

Transient waves with zonal wavenumber 2 ($s = 2$ TWs) have the second largest amplitude among planetary waves in the SH middle stratosphere (Randel 1988; Harvey et al. 2002). The amplitude of $s = 2$ TWs attains its maximum in the austral spring (Randel 1988; Manney et al. 1991a). Scinocca and Haynes (1998) proposed the generation mechanism for $s = 2$ TWs in terms of nonlinear wave-wave interaction of baroclinic eddies in the troposphere. They indicated using model simulations that high-frequency forcing with dominant $s = 2$ structure organized by synoptic-scale waves is responsible for $s = 2$ higher-frequency disturbances observed in the real SH stratosphere. On the other hand, Manney et al. (1991b) paid attention to the confined structure of $s = 2$ TWs in the stratosphere and suggested that in situ instability is responsible for their generation. They showed using a linear QG model that unstable modes with zonal wavenumber 2 have similar periods and spatial structures to observations.

As discussed above, climatology of planetary waves in the SH stratosphere has

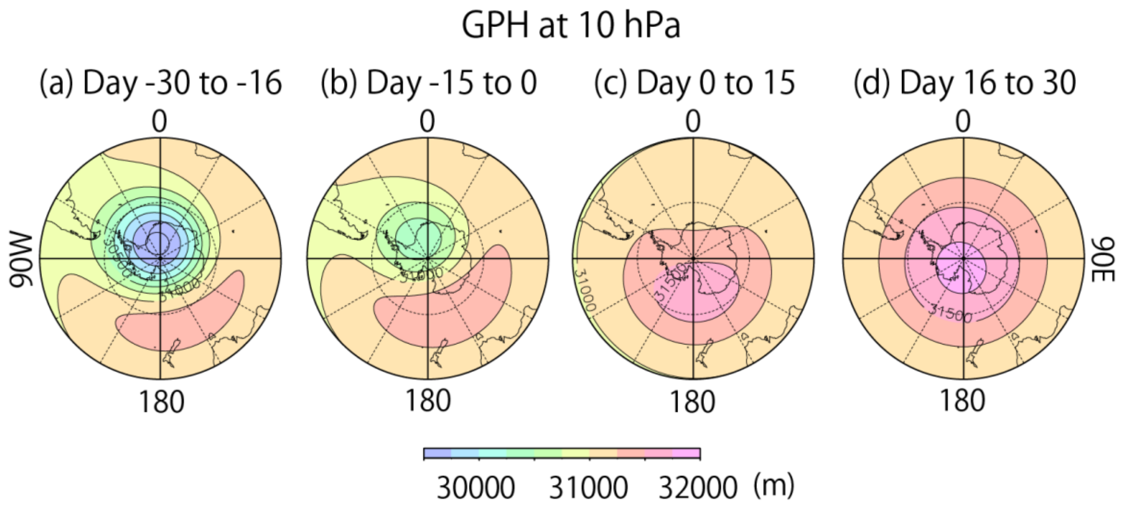

Fig. 1.3 Polar stereographic projection maps of GPH composites at 10 hPa with respect to the onset of SFW (day 0) for (a) day -30 to -16, (b) day -15 to 0, (c) day 0 to 15, and (d) day 16 to 30. MERRA-2 from 1980 to 2017 are used.

already been shown by previous studies. However, time period of data used for the climatology is relatively short: for example, 8 and 12 years in Randel (1988) and Quintanar and Mechoso (1995a), respectively. Short time period of analysis may lead to spurious climatological seasonal evolution if, for example, sporadic events with extreme amplitudes of planetary waves occur. In addition, it is still unclear how climatological seasonal evolution of amplitudes of stratospheric planetary waves is related to wave transmission properties of the mean flow and amplitudes of planetary waves in the troposphere.

1.2 Stratospheric final warming

In the polar stratosphere, winter terminates with breakdown of the polar vortex called SFW, as mentioned in section 1.1. During SFWs, the polar vortex decays and its center moves away from the Pole. On the other hand, an anticyclone called the Australian High in the SH (Harvey et al. 2002) develops to the south of Australia and moves to the South Pole (Fig. 1.3; Hirano et al. 2016). SFWs can impact tropospheric

インターネット公表に対する著作権者からの許諾が得られていないため非公開

circulation (Sun and Robinson 2009; Sun et al. 2011; Byrne and Shepherd 2018; Lim et al. 2018). Black and McDaniel (2007b) found that geopotential height (GPH) anomalies from their climatology in the lower troposphere have characteristic longitudinal structures which exhibit much more asymmetry than the southern annular mode pattern at early and late stages of SFWs in the SH (Fig. 1.4).

In the SH, timing of SFW is later in late 1990s than in late 1970s (Fig. 3.1) mainly because of stratospheric ozone loss (Waugh et al. 1999; Zhou et al. 2000; Karpechko et al. 2005; Langematz and Kunze 2006; Haigh and Roscoe 2009). After around 2000, however, there is a slightly negative trend in timing of SFW (Fig. 3.1) probably as a response to ozone recovery (Newman et al. 2006; Yang et al. 2008; Salby et al. 2012; Wilcox and Charlton-Perez 2013). In addition to these trends, interannual variability of timing of SFW associated with that of wave activity is observed (Fig. 3.1; Hio and Yoden 2005; Hirano et al. 2016). Hirano et al. (2016) showed that the timing of SFW is significantly related with polar temperature and the vertical component of Eliassen-Palm (E-P) flux in the lower stratosphere during the austral spring. Furthermore, using a formulae of three-dimensional residual mean flow (Kinoshita and Sato 2013a), they revealed zonally asymmetric structure of adiabatic heating by residual mean flow.

In the SH upper troposphere, $s = 1$ QSWs have the largest amplitude among planetary stationary waves in the extratropics (Turner et al. 2017). It was indicated by model simulations that tropospheric $s = 1$ QSWs at southern high latitudes are predominantly generated at low latitudes in perpetual-October mode (Quintanar and Mechoso 1995b). Inatsu and Hoskins (2004) suggested that zonal asymmetry in tropical sea surface temperature (SST) contributes to formation of wintertime extratropical stationary waves in the SH. On interannual time scales, previous studies pointed out that tropical SST variability can influence the polar stratospheric wave activity and temperature in both hemispheres. Especially, the influence of canonical El Niño–Southern Oscillation (ENSO) and central Pacific ENSO, when eastern and central Pacific SST anomalies, respectively, are observed, has been investigated so far (Domeisen et al. 2019). In the SH, Hurwitz et al. (2011) compared responses of stratospheric temperature to the two types of ENSO during the austral spring, and showed that polar temperature in the lower stratosphere is higher during the central Pacific El Niño, while the canonical El Niño does not significantly impact the stratospheric temperature. On the other hand, Lin et al. (2012) found that enhanced (suppressed) stratospheric planetary-wave activity is associated with the canonical La Niña- (El Niño-) like and the central Pacific El Niño- (La Niña-) like SST patterns. Moreover, previous studies dealing with the stratospheric responses to tropical SST found Rossby wavetrain-like features propagating from lower to higher latitudes. However, detailed tropospheric conditions leading to earlier SFWs are still not elucidated well.

1.3 Purpose of this study

As mentioned in sections 1.1 and 1.2, it is still not clear how climatology and interannual variability of planetary waves in the SH stratosphere are related to tropospheric circulation. The present study will investigate climatology and interannual variability of planetary-wave amplitudes in the stratosphere and their connection to tropospheric planetary waves. Characteristics in the upper stratosphere and lower mesosphere, which are rarely featured in previous studies due to limited availability of data, are also revealed.

The thesis is organized as follows. In chapter 2, climatology of planetary-wave amplitudes in the SH stratosphere is shown using reanalysis data for 38 years as a function of calendar months and height. The climatology is then compared to that shown by previous studies such as Randel (1988) and Quintanar and Mechoso (1995a). In order to examine cause of the climatological seasonal evolution of planetary-wave amplitudes in the stratosphere, the relation with tropospheric planetary-wave amplitudes and wave transmission properties of the mean flow through which planetary waves propagate is investigated. The wave transmission properties of the mean flow are diagnosed by refractive index squared. Relation of distribution of refractive index squared with structure of the polar night jet is also discussed. Chapter 3 deals with interannual variability of timing of SFWs. As mentioned earlier, the relation between timing of SFW and stratospheric wave activity on interannual time scales has already been confirmed (Hio and Yoden 2005; Hirano et al. 2016). The amplitude of $s = 1$ QSWs is the largest among extratropical planetary waves in the SH stratosphere, and attains a maximum in the austral spring (Randel 1988; Quintanar and Mechoso 1995a).

Thus, interannual variability of timing of SFW in the SH is investigated in terms of amplitudes of stratospheric and tropospheric $s = 1$ QSWs. Wave transmission properties of the mean flow through which $s = 1$ stationary waves propagate are also examined. Next, the mechanism in modulation of tropospheric $s = 1$ QSW amplitudes is explored. Considering that it is confirmed that main source of tropospheric $s = 1$ QSWs is at low latitudes (Quintanar and Mechoso 1995b), the analysis is focused on remote $s = 1$ responses at high latitudes to tropical heating and midlatitude background flow in the upper troposphere during the austral spring. The present study will employ a linear barotropic model, which has been confirmed to qualitatively well reproduce steady extratropical responses to tropical heating in the literature (Hoskins and Ambrizzi 1993; Ambrizzi et al. 1995; Ting 1996; Ambrizzi and Hoskins 1997; Watanabe 2004). It should be noted that the strongest teleconnection between the tropics and southern high latitudes in the upper troposphere is observed during the austral spring (Jin and Kirtman 2009; 2010; Schneider et al. 2012; Yuan et al. 2018). Summary and concluding remarks are given in chapter 4

1.4 Data description

Three-hourly three-dimensional wind, GPH, temperature, ozone mass mixing ratio, and temperature tendency due to longwave and shortwave radiation, and moist processes from the Modern-Era Retrospective Analysis for Research and Applications, Version 2 (MERRA-2; Gelaro et al. 2017) covering the period of 38 years (1980–2017) are used. The data are provided for 42 pressure levels from 1000 hPa to 0.1 hPa with a horizontal interval of 1.25°. Daily SST from Optimum Interpolation Sea Surface Temperature (OISST; Reynolds et al. 2007; Banzon et al. 2016) with a horizontal interval of 0.25° from September 1981 to December 2017 and daily outgoing longwave

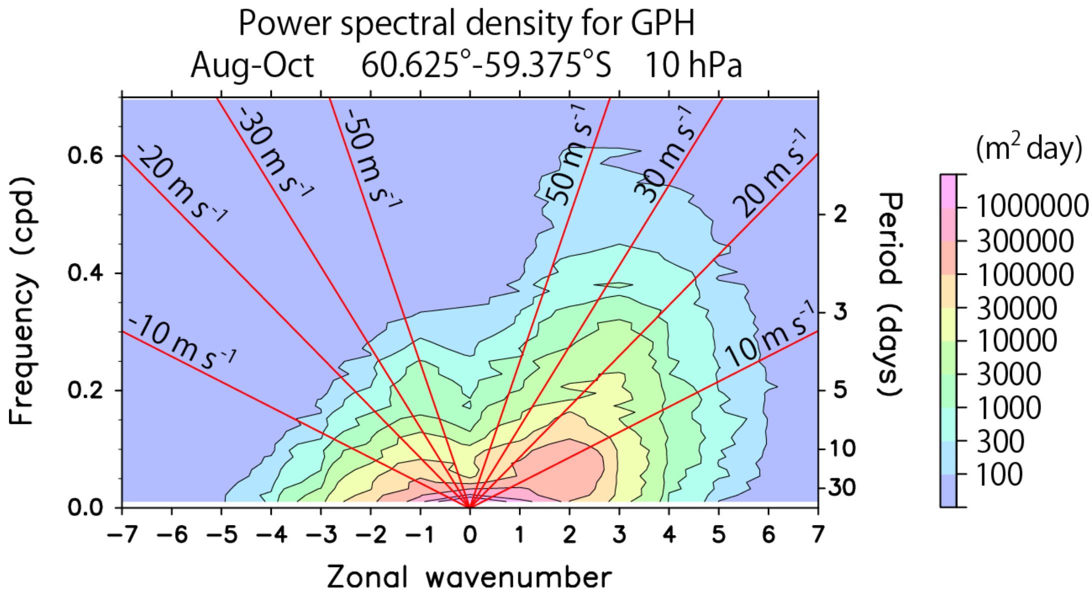

Fig. 1.4 Climatology of power spectral density for GPH at 10 hPa during August–October averaged over 60.625°–59.375°S. Contours representing 100, 300, 1000, 3000, 10000, 30000, 100000, 300000, 1000000, and 3000000 $\mathrm{m^2}$ day are drawn. Red lines denote ground-based eastward phase speed.

radiation (OLR) from NOAA Interpolated OLR (Liebmann and Smith 1996) with a horizontal interval of 2.5° from January 1980 to January 2017 are also used.

1.5 Definitions of quasi-stationary and transient waves

In this study, QSWs and TWs are defined as components with wave periods longer than 30 days and those from 5 to 30 days, respectively (Randel 1988; Harvey et al. 2002). Figure 1.4 shows climatology of power spectral density for GPH at 10 hPa. A distinct peak is observed for $|s| \leq 1$ and wave periods longer than 30 days. For $s = 2$ and 3, eastward traveling waves with zonal phase speed smaller than $20\ \mathrm{m\ s^{-1}}$ are dominant. The power spectral density for $s \geq 4$ is weaker for larger zonal wavenumber. The above features are consistent with previous studies. Especially, QSWs and TWs defined in this study are the most prominent for $s = 1$ and $s = 2$, respectively.

Chapter 2
Climatology of stratospheric planetary waves in the SH and their tropospheric origins

Climatology of planetary-wave amplitudes in the SH stratosphere has already been shown by previous studies. However, time period of data used for the climatology is relatively short: for example, 8 and 12 years in Randel (1988) and Quintanar and Mechoso (1995a), respectively. Short time period of analysis may lead to spurious climatological seasonal evolution if, for example, sporadic events with extreme amplitudes of planetary waves occur. In this chapter, using reanalysis data for 38 years from 1980 to 2017, climatological seasonal evolution of planetary-wave amplitudes in the SH stratosphere is shown in order to update it. The climatology for 38 years is compared to that shown by the previous studies. The mechanism causing the seasonal variation of stratospheric planetary-wave amplitudes is examined. First, the relation with seasonal evolution of tropospheric planetary-wave amplitudes is examined. Wave transmission properties of the mean flow also affect amplitudes of stratospheric planetary waves. To diagnose it, distribution of refractive index squared is examined. Relation of the distribution of refractive index squared with structure of the polar night jet is also discussed. Results of the analysis for $s = 1$ QSWs and $s = 2$ TWs, whose amplitudes are the largest among stratospheric planetary waves in the SH, are shown.

本章については、5 年以内に雑誌等で刊行される予定であるため、以降の節について、非公開。

Chapter 3
Interannual variability of SFW in the SH and its connection to the troposphere

It has already been confirmed by previous studies that SFWs occur earlier when stratospheric wave activity is larger. However, dominant component of the stratospheric waves which contributes to the interannual variability of timing of SFW is not clear. Moreover, detailed tropospheric conditions leading to earlier SFWs are still not elucidated well. The amplitude of $s = 1$ QSWs is the largest among extratropical planetary waves in the SH stratosphere, and attains a maximum in the austral spring, as shown in chapter 2. Thus, interannual variability of timing of SFW in the SH is investigated in terms of stratospheric and tropospheric $s = 1$ QSW amplitudes, and wave transmission properties of the mean flow. The mechanism in modulation of $s = 1$ QSW amplitudes in the troposphere is also explored using a linear barotropic model in addition to reanalysis data. The analysis of tropospheric $s = 1$ QSWs is focused on the influence of tropical heating and midlatitude background flow in the upper troposphere.

本章については、5 年以内に雑誌等で刊行される予定であるため、以降の節について、非公開。

Chapter 4
Summary and concluding remarks

本章については、5 年以内に雑誌等で刊行される予定であるため、非公開。

Acknowledgements

First of all, I would particularly like to express my gratitude to my supervisor Prof. K. Sato. My dissertation committee members Profs. H. Nakamura, T. Hibiya, K. Iga, and M. Watanabe provided many valuable comments and suggestions. I also thank M. Koike, T. Tozuka, H. Miura, and K. Kohma for many useful comments and discussions. I appreciate Dr. K. Nishii at Mie University for many fruitful comments and helping with application of the wave activity flux for quasi-stationary waves, and Dr. T. Kinoshita at Japan Agency for Marine-Earth Science and Technology for instructing how to calculate and interpret the wave activity flux for synoptic-scale waves. The linear barotropic model is provided by Dr. M. Hayashi at University of Hawaii and Prof. M. Watanabe at Atmosphere and Ocean Research Institute, the University of Tokyo. I would also like to express my gratitude to Dr. K. Kodera at Meteorological Research Institute, Dr. Seok-Woo Son at Seoul national University, Dr. Y. Tomikawa at National Institute of Polar Research, and Dr. S. Noguchi at Japan Agency for Marine-Earth Science and Technology for their suggestive comments. Special thanks are given to colleagues and former members in the atmospheric dynamics laboratory: Dr. Y. Sumi, Dr. M. Mihalikova, Dr. K. Okamoto, Dr. C. Tsuchiya, Dr. M. Nomoto, Dr. Y. Yasuda, Dr. R. Shibuya, Dr. A. Amemiya, Mr. A. Masuda, Mr. R. Yasui, Mr. Y. Hayashi, Mr. Y. Minamihara, Mr. D. Koshin, Mr. S. Nakajima, Mr. Y. Matsushita, Ms. H. Okui, Mr. M. Mizukoshi.

All figures in the present study are depicted by using Dennou Club Library. MERRA-2 data are provided by https://disc.gsfc.nasa.gov/daac-bin/FTPSubset2.pl?LOOKUPID_List=M2I3NPASM. OISST data are provided by https://www.ncdc.noaa.gov/oisst/data-access. Interpolated OLR data are provided by the NOAA/OAR/ESRL PSD, Boulder, Colorado, USA, from their Web site at https://www.esrl.noaa.gov/psd/. This work is supported by JST CREST

Grant Number JPMJCR1663.

Finally, I really appreciate support and encouragement from my family and friends.

References

Alexander, M. J., S. D. Eckermann, D. Broutman, and J. Ma, 2009: Momentum flux estimates for South Georgia Island mountain waves in the stratosphere observed via satellite. *Geophys. Res. Lett.,* **36,** L12816.

Ambrizzi, T., and B. J. Hoskins, 1997: Stationary Rossby-wave propagation in a baroclinic atmosphere. *Quart. J. Roy. Meteor. Soc.,* **123,** 919–928.

——, ——, and H-H Hsu, 1995: Rossby wave propagation and teleconnection patterns in the austral winter. *J. Atmos. Sci.,* **52,** 3661–3672.

Amemiya, A., and K. Sato, 2016: A new gravity wave parameterization including three-dimensional propagation. *J. Meteorol. Soc. Jpn.,* **94,** 237–256.

Andrews, D. G., and M. E. McIntyre, 1976: Planetary waves in horizontal and vertical shear: The generalized Eliassen-Palm relation and the mean zonal acceleration. *J. Atmos. Sci.,* **33,** 2031–2048.

——, and ——, 1978: Generalized Eliassen-Palm and Charney-Drazin theorems for waves on axisymmetric mean flows in compressible atmospheres. *J. Atmos. Sci.,* **35,** 175–185.

——, J. R. Holton, and C. B. Leovy, 1987: *Middle Atmosphere Dynamics.* 489 pp.

Anstey, J. A., and T. G. Shepherd, 2014: High-latitude influence of the quasi-biennial oscillation. *Quart. J. Roy. Meteor. Soc.,* **140,** 1–21.

Baldwin, M. P., and T. J. Dunkerton, 1998: Quasi-biennial modulation of the southern hemisphere stratospheric polar vortex. *Geophys. Res. Lett.* **25,** 3343–3346.

——, and Coauthors, 2001: The quasi-biennial oscillation. *Rev. Geophys.,* **39,** 179–229.

Banzon, V., T. M. Smith, T. M. Chin, C. Liu, and W. Hankins, 2016: A long-term record of blended satellite and in situ sea-surface temperature for climate monitoring, modeling and environmental studies. *Earth Syst. Sci. Data*, **8**, 165–176.

Black, R. X., and B. A. McDaniel, 2007a: The dynamics of Northern Hemisphere stratospheric final warming events. *J. Atmos. Sci.,* **64,** 2932–2946.

——, and ——, 2007b: Interannual variability in the Southern Hemisphere circulation organized by stratospheric final warming events. *J. Atmos. Sci.,* **64,** 2968–2974.

——, ——, and W. A. Robinson, 2006: Stratosphere-troposphere coupling during spring onset. *J. Climate,* **19,** 4891–4901.

Butchart, N., and Coauthors, 2011: Multimodel climate and variability of the stratosphere. *J. Geophys. Res.,* **116,** D05102.

Butler, A. H., J. P. Sjoberg, D. J. Seidel, and K. H. Rosenlof, 2017: A sudden stratospheric warming compendium. *Earth Syst. Sci. Data,* **9,** 63–76.

Byrne, N. J., and T. G. Shepherd, 2018: Seasonal persistence of circulation anomalies in the Southern Hemisphere stratosphere and its implications for the troposphere. *J. Climate,* **31,** 3467–3483.

Cai, M., and M. Mak, 1990: Symbiotic relation between planetary and synoptic scale waves. *J. Atmos. Sci.,* **47,** 2953–2968.

Chang, E. K. M., S. Lee, and K. L. Swanson, 2002: Storm track dynamics. *J. Climate,* **15,** 2163–2183.

Charlton, A. J., and L. M. Polvani, 2007: A new look at stratospheric sudden warmings. Part I: Climatology and modeling benchmarks. *J. Climate,* **20,** 449–469.

——, A. O'Neill, W. Lahoz, and P. Berrisford, 2005: The splitting of the stratospheric polar vortex in the Southern Hemisphere, September 2002: Dynamical evolution. *J. Atmos. Sci.,* **62,** 590–602.

Charney, J. G., and P. G. Drazin, 1961: Propagation of planetary-scale disturbances from the lower into the upper atmosphere. *J. Geophys. Res.,* **66,** 83–109.

De la Cámara, A., F. Lott, V. Jewtoukoff, R. Plougonven, and A. Hertzog, 2016: On the gravity wave forcing during the southern stratospheric final warming in LMDZ. *J. Atmos. Sci.,* **73,** 3213–3226.

Domeisen, D. I. V., C. I. Garfinkel, and A. H. Butler, (2019): The teleconnection of El Niño Southern Oscillation to the stratosphere. *Rev. Geophys.,* **57,** 5–47.

Eyring, V., and Coauthors, 2006: Assessment of temperature, trace species, and ozone in chemistry-climate model simulations of the recent past. *J. Geophys. Res.,* **111,** D22308.

Garfinkel, C. I., and D. L. Hartmann, 2008: Different ENSO teleconnections and their effects on the stratospheric polar vortex. *J. Geophys. Res.,* **113,** D18114.

——, and L. D. Oman, 2018: Effect of gravity waves from small islands in the Southern Ocean on the Southern Hemisphere atmospheric circulation. *J. Geophys. Res. Atmos.,* **123,** 1552–1561.

——, D. L. Hartmann, and F. Sassi, 2010: Tropospheric precursors of anomalous Northern Hemisphere stratospheric polar vortices. *J. Climate,* **23,** 3282–3299.

——, L. D. Oman, E. A. Barnes, D. W. Waugh, M. H. Hurwitz, and A. M. Molod, 2013: Connections between the spring breakup of the Southern Hemisphere polar vortex, stationary waves, and air–sea roughness. *J. Atmos. Sci.,* **70,** 2137–2151.

Gelaro, R., and Coauthors, 2017: The Modern-Era Retrospective Analysis for Research and Applications, version 2 (MERRA-2). *J. Climate,* **30,** 5419–5454.

Haigh, J. D., and H. K. Roscoe, 2009: The final warming date of the Antarctic polar vortex and influences on its interannual variability. *J. Climate,* **22,** 5809–5819.

Harvey, V. L., R. B. Pierce, T. D. Fairlie, and M. H. Hitchman, 2002: A climatology of stratospheric polar vortices and anticyclones. *J. Geophys. Res.,* **107,** 4442.

Hegyi, B. M., and Y. Deng, 2011: A dynamical fingerprint of tropical Pacific sea surface temperatures on the decadal-scale variability of cool-season arctic precipitation. *J.*

Geophys. Res., **116,** D20121.

Hio, Y., and S. Yoden, 2005: Interannual variations of the seasonal march in the Southern Hemisphere stratosphere for 1979–2002 and characterization of the unprecedented year 2002. *J. Atmos. Sci.,* **62,** 567–580.

Hirano, S., M. Kohma, and K. Sato, 2016: A three-dimensional analysis on the role of atmospheric waves in the climatology and interannual variability of stratospheric final warming in the Southern Hemisphere. *J. Geophys. Res. Atmos.,* **121,** 8429–8443.

Hirota, I., T. Hirooka, and M. Shiotani, 1983: Upper stratospheric circulations in the two hemispheres observed by satellites. *Quart. J. Roy. Meteor. Soc.,* **109,** 443–454.

Holton, J. R., and H.-C. Tan, 1980: The influence of the equatorial quasi-biennial oscillation on the global circulation at 50 mb. *J. Atmos. Sci.,* **37,** 2200–2208.

Horel, J. D., and J. M. Wallace, 1981: Planetary-scale atmospheric phenomena associated with the Southern Oscillation. *Mon. Wea. Rev.,* **109,** 813–829.

Hoskins, B. J., and D. J. Karoly, 1981: The steady linear response of a spherical atmosphere to thermal and orographic forcing. *J. Atmos. Sci.,* **38,** 1179–1196.

——, and P. D. Sardeshmukh, 1988: Generation of global rotational flow by steady idealized tropical divergence. *J. Atmos. Sci.,* **45,** 1228–1251.

——, and T. Ambrizzi, 1993: Rossby wave propagation on a realistic longitudinally varying flow. *J. Atmos. Sci.,* **50,** 1661–1671.

Hu, J., R. Ren, and H. Xu, 2014: Occurrence of winter stratospheric sudden warming events and the seasonal timing of spring stratospheric final warming. *J. Atmos. Sci.,* **71,** 2319–2334.

Hurwitz, M. M., P. A. Newman, L. D. Oman, and A. M. Molod, 2011: Response of the Antarctic stratosphere to two types of El Niño events. *J. Atmos. Sci.,* **68,** 812–822.

——, ——, F. Li, L. D. Oman, O. Morgenstern, P. Braesicke, and J. A. Pyle, 2010:

Assessment of the breakup of the Antarctic polar vortex in two new chemistry-climate models. *J. Geophys. Res.,* **115,** D07105

Inatsu, M., and B. J. Hoskins, 2004: The zonal asymmetry of the Southern Hemisphere winter storm track. *J. Climate,* **17,** 4882–4892.

Jin, D., and B. P. Kirtman, 2009: Why the Southern Hemisphere ENSO responses lead ENSO. *J. Geophys. Res.,* **114,** D23101.

——, and ——, 2010: How the annual cycle affects the extratropical response to ENSO. *J. Geophys. Res.,* **115,** D06102.

Karoly, D. J., 1983: Rossby wave propagation in a barotropic atmosphere. *Dyn, Atmos. Oceans,* **7,** 111–125.

Karpechko, A. Y., E. Kyrö, and B. M. Knudsen, 2005: Arctic and Antarctic polar vortices 1957–2002 as seen from the ERA-40 reanalyses. *J. Geophys. Res.,* **110,** D21109.

Kidson, J. W., 1988: Indices of the Southern Hemisphere zonal wind. *J. Climate,* **1,** 183–194.

Kinoshita, T., and K. Sato, 2013a: A formulation of three-dimensional residual-mean flow applicable both to inertia-gravity waves and to Rossby waves. *J. Atmos. Sci.,* **70,** 1577–1602.

——, and ——, 2013b: A formulation of unified three-dimensional wave activity flux of inertia-gravity waves and Rossby waves. *J. Atmos. Sci.,* **70,** 1603–1615.

Krüger, K., B. Naujokat, and K. Labitzke, 2005: The unusual midwinter warming in the Southern Hemisphere stratosphere 2002: A comparison to Northern Hemisphere phenomena. *J. Atmos. Sci.,* **62,** 603–613.

Labitzke, K., 1980: Climatology of the stratosphere and mesosphere. *Philos. Trans. Roy. Soc. London,* **A296,** 7–18.

Langematz, U., and M. Kunze, 2006: An update on dynamical changes in the Arctic and

Antarctic stratospheric polar vortices. *Climate Dyn.,* **27,** 647–660.

Leovy, C. B., and P. J. Webster, 1976: Stratospheric long waves: Comparison of thermal structure in the Northern and Southern Hemispheres. *J. Atmos. Sci.,* **33,** 1624–1638.

Li, X., E. P. Gerber, D. M. Holland, and C. Yoo, 2015: A Rossby wave bridge from the tropical Atlantic to West Antarctica. *J. Climate,* **28,** 2256–2273.

Liebmann, B., and C. A. Smith, 1996: Description of a complete (interpolated) outgoing longwave radiation dataset. *Bull. Amer. Meteor. Soc.,* **77,** 1275–1277.

Lim, E.-P., H. H. Hendon, and D. W. J. Thompson, 2018: On the seasonal evolution and impacts of stratosphere-troposphere coupling in the Southern Hemisphere. *J. Geophys. Res. Atmos.,* **123,** 12002–12016.

Lin, P., Q. Fu, and D. L. Hartmann, 2012: Impact of tropical SST on stratospheric planetary waves in the Southern Hemisphere. *J. Climate,* **25,** 5030–5046.

Manney, G. L., J. D. Farrara, and C. R. Mechoso, 1991a: The behavior of wave 2 in the Southern Hemisphere stratosphere during late winter and early spring. *J. Atmos. Sci.,* **48,** 976–998.

——, C. R. Mechoso, L. S. Elson, and J. D. Farrara, 1991b: Planetary-scale waves in the Southern Hemisphere winter and early spring stratosphere: Stability analysis. *J. Atmos. Sci.,* **48,** 2509–2523.

Matsuno, T., 1970: Vertical propagation of stationary planetary waves in the winter Northern Hemisphere. *J. Atmos. Sci.,* **27,** 871–883.

Matthewman, N., J. Esler, A. Charlton-Perez, and L. Polvani, 2009: A new look at stratospheric sudden warmings. Part III: Polar vortex evolution and vertical structure. *J. Climate,* **22,** 1566–1585.

McLandress, C., and T. G. Shepherd, S. Polavarapu, and S. R. Beagley, 2012: Is missing orographic gravity wave drag near 608S the cause of the stratospheric zonal wind biases in chemistry–climate models? *J. Atmos. Sci.,* **69,** 802–818.

Mitchell, D. M., L. J. Gray, J. Anstey, M. P. Baldwin, and A. J. Charlton-Perez, 2013: The influence of stratospheric vortex displacements and splits on surface climate. *J. Climate,* **26,** 2668–2682.

Naito, Y., 2002. Planetary wave diagnostics on the QBO effects on the deceleration of the polar-night jet in the southern hemisphere. *J. Meteor. Soc. Jpn.,* **80,** 985–995.

Nakamura, H., and A. Shimpo, 2004: Seasonal variations in the Southern Hemisphere storm tracks and jet stream as revealed in a reanalysis dataset. *J. Climate,* **17,** 1828–1844.

——, M. Tanaka, and J. M. Wallace, 1987: Horizontal structure and energetics of Northern Hemisphere wintertime teleconnection patterns. *J. Atmos. Sci.,* **44,** 3377–3391.

Newman, P. A., and E. R. Nash, 2005: The unusual Southern Hemisphere stratosphere winter of 2002. *J. Atmos. Sci.,* **62,** 614–628.

——, ——, S. R. Kawa, S. A. Montzka, and S. M. Schauffler, 2006: When will the Antarctic ozone hole recover? *Geophys. Res. Lett.,* **33,** L12814.

Palmeiro, F. M., D. Barriopedro, R. García-Herrera, and N. Calvo, 2015: Comparing sudden stratospheric warming definitions in reanalysis data. *J. Climate,* **28,** 6823–6840.

Pitts, M. C., L. R. Poole, and R. Gonzalez, 2018: Polar stratospheric cloud climatology based on CALIPSO spaceborne lidar measurements from 2006 to 2017. *Atmos. Chem. Phys.,* **18,** 10881–10913.

Plumb, R. A., 1985: On the three-dimensional propagation of stationary waves. *J. Atmos. Sci.,* **42,** 217–229.

——, 2002: Stratospheric transport. *J. Meteorol. Soc. Jpn.*, **80**, 793–809.

Quintanar, A. I., and C. R. Mechoso, 1995a: Quasi-stationary waves in the Southern

Hemisphere. Part I: Observational data. *J. Climate,* **8,** 2659–2672.

——, and ——, 1995b: Quasi-stationary waves in the Southern Hemisphere. Part II: Generation mechanisms. *J. Climate,* **8,** 2673–2690.

Randel, W. J., 1988: The seasonal evolution of planetary waves in the southern hemisphere stratosphere and troposphere. *Quart. J. Roy. Meteor. Soc.,* **114,** 1385–1409.

Reynolds, R. W., T. M. Smith, C. Liu, D. B. Chelton, K. S. Casey, and M. G. Schlax, 2007: Daily high-resolution-blended analyses for sea surface temperature. *J. Climate*, **20,** 5473–5496.

Roscoe, H. K., J. D. Shanklin, and S. R. Colwell, 2005: Has the Antarctic vortex split before 2002? *J. Atmos. Sci.,* **62,** 581–588.

Salby, M. L., E. A. Titova, and L. Deschamps, 2012: Changes of the Antarctic ozone hole: Controlling mechanisms, seasonal predictability, and evolution. *J. Geophys. Res.,* **117,** D10111.

Sato, K., S. Watanabe, Y. Kawatani, Y. Tomikawa, K. Miyazaki, and M. Takahashi, 2009: On the origins of mesospheric gravity waves. *Geophys. Res. Lett.,* **36,** L19801.

Scheffler, G., and M. Pulido, 2015: Compensation between resolved and unresolved wave drag in the stratospheric final warmings of the Southern Hemisphere. *J. Atmos. Sci.,* **72,** 4393–4411.

Schneider, D. P., Y. Okumura, and C. Deser, 2012: Observed Antarctic interannual climate variability and tropical linkages. *J. Climate,* **25,** 4048–4066.

Scinocca, J. F., and P. H. Haynes, 1998: Dynamical forcing of stratospheric planetary waves by tropospheric baroclinic eddies. *J. Atmos. Sci.,* **55,** 2361–2392.

Scott, R. K., and P. H. Haynes, 2002: The seasonal cycle of planetary waves in the winter stratosphere. *J. Atmos. Sci.,* **59,** 803–822.

Shimizu, M. H., and I. F. de Albuquerque Cavalcanti, 2011: Variability patterns of Rossby wave patterns. *Climate Dyn.,* **37,** 441–454.

Simmons, A. J., J. M. Wallace, and G. W. Branstator, 1983: Barotropic wave propagation and instability, and atmospheric teleconnection patterns. *J. Atmos. Sci.,* **40,** 1363–1392.

Solomon, S., 1999: Stratospheric ozone depletion: A review of concepts and history. *Rev. Geophys.,* **37,** 275–316.

Sun, L., and W. A. Robinson, 2009: Downward influence of stratospheric final warming events in an idealized model. *Geophys. Res. Lett.,* **36,** L03819.

——, ——, and G. Chen, 2011: The role of planetary waves in the downward influence of stratospheric final warming events. *J. Atmos. Sci.,* **68,** 2826–2843.

Sutherland, B. R., U. Achatz, P. C. Colm-cille, and J. M. Klymak, 2019: Recent progress in modeling imbalance in the atmosphere and ocean. *Phys. Rev. Fluids,* **4,** 010501.

Takaya, K., and H. Nakamura, 2001: A formulation of a phase independent wave-activity flux for stationary and migratory quasigeostrophic eddies on a zonally varying basic flow. *J. Atmos. Sci.,* **58,** 608–627.

Tanaka, S., K. Nishii, and H. Nakamura, 2016: Vertical structure and energetics of the western Pacific teleconnection pattern. *J. Climate,* **29,** 6597–6616.

Ting, M., 1996: Steady linear response to tropical heating in barotropic and baroclinic models. *J. Atmos. Sci.,* **53,** 1698–1709.

Turner, J., J. S. Hosking, T. J. Bracegirdle, T. Phillips, and G. J. Marshall, 2017: Variability and trends in the Southern Hemisphere high latitude, quasi-stationary planetary waves. *Int. J. Climatol.* **37,** 2325–2336.

Wakata, Y., and M. Uryu, 1987: Stratospheric multiple equilibria and seasonal variations. *J. Meteorol. Soc. Jpn.*, **65,** 27–42.

Watanabe, M., 2004: Asian jet waveguide and a downstream extension of the North Atlantic Oscillation. *J. Climate,* **17,** 4674–4691.

Waugh, D. W., W. J. Randel, S. Pawson, P. A. Newman, and E. R. Nash, 1999: Persistence of the lower stratospheric polar vortices. *J. Geophys. Res.,* **104,** 27191–27202.

Wilcox, L. J., and A. J. Charlton-Perez, 2013: Final warming of the Southern Hemisphere polar vortex in high- and low-top CMIP5 models. *J. Geophys. Res. Atmos.,* **118,** 2535–2546.

Wirth, V., 1991: What causes the seasonal cycle of stationary waves in the southern stratosphere? *J. Atmos. Sci.,* **48,** 1194–1200.

Yang, E.-S., D. M. Cunnold, M. J. Newchurch, R. J. Salawitch, M. P. McCormick, J. M. Russell III, J. M. Zawodny, and S. J. Oltmans, 2008: First stage of Antarctic ozone recovery. *J. Geophys. Res.,* **113,** D20308.

Yoden, S., 1987: A new class of stratospheric vacillations in a highly truncated model due to wave interference. *J. Atmos. Sci.,* **44,** 3696–3709.

Yuan, X., M. R. Kaplan, and M. A. Cane, 2018: The interconnected global climate system—a review of tropical–polar teleconnections. *J. Climate*, **31,** 5765–5792.

Zhou, S. T., M. E. Gelman, A. J. Miller, and J. P. McCormack, 2000: An inter-hemisphere comparison of the persistent stratospheric polar vortex. *Geophys. Res. Lett.,* **27,** 1123–1126.